Vol 17 No 7, July 2008
1674-1056/2008/17(07)/2646-09

Chinese Physics B

© 2008 Chin. Phys. Soc.
and IOP Publishing Ltd

High density gas state at water/graphite interface studied by molecular dynamics simulation*

Wang Chun-Lei(王春雷)[a)b)], Li Zhao-Xia(李朝霞)[a)b)], Li Jing-Yuan(李敬源)[c)], Xiu Peng(修 鹏)[a)d)], Hu Jun(胡 钧)[a)e)], and Fang Hai-Ping(方海平)[a)†]

[a)] *Shanghai Institute of Applied Physics, Chinese Academy of Sciences, Shanghai* 201800, *China*
[b)] *Graduate School of the Chinese Academy of Sciences, Beijing* 100080, *China*
[c)] *Department of Physics, Zhejiang University, Hangzhou* 310027, *China*
[d)] *School of Physics and Microelectronics, Shandong University, Jinan* 250100, *China*
[e)] *Bio-X Life Sciences Research Center, College of Life Science and Technology, Shanghai Jiaotong University, Shanghai* 200030, *China*

(Received 13 September 2007; revised manuscript received 6 November 2007)

In this paper molecular dynamics simulations are performed to study the accumulation behaviour of N_2 and H_2 at water/graphite interface under ambient temperature and pressure. It finds that both N_2 and H_2 molecules can accumulate at the interface and form one of two states according to the ratio of gas molecules number to square of graphite surface from our simulation results: gas films (pancake-like) for a larger ratio and nanobubbles for a smaller ratio. In addition, we discuss the stabilities of nanobubbles at different environment temperatures. Surprisingly, it is found that the density of both kinds of gas states can be greatly increased, even comparable with that of the liquid N_2 and liquid H_2. The present results are expected to be helpful for the understanding of the stable existence of gas film (pancake-like) and nanobubbles.

Keywords: nanobubbles and gas film, hydrophobic interface, molecular dynamics simulations, high density

PACC: 6800, 6810J, 0155

1. Introduction

The nature of the long-ranged hydrophobic force at the interface between water and hydrophobic surface is a subject of intense interest and hot debates all along for a long time.[1−7] It is believed that hydrophobic interactions are involved in diverse phenomena including protein folding, amphiphathic molecule self-assembly, membrane fusion, oil dispersion and mineral floatation.[8] It is still not possible to understand why there is such a long-ranged attractive force from the classical DLVO theory.[9] The hypothesis of the existence of sub-microscopic gas bubbles on solid surfaces immersed in water was first proposed to account for this unexpected long-ranged attractive force between hydrophobic surfaces.[10−13] Since then, a range of experimental evidences has been presented in support of the existence of nanobubbles at water/hydrophobic interface, including direct imaging of nanobubbles by tapping mode atomic force microscopy (AFM),[5,13−19] rapid cryofixation-freeze fracture[20] and neutron reflectometry.[21] It was newly reported that hydrogen nanobubbles were controllably produced on graphite surface using electrochemical approach, which further approved the real existence of nanobubbles.[22] On the other hand, some experiments detected a thin water layer of density deficit approximately several nanometres by neutron and x-ray reflectivity, which predicted the existence of gas film.[23,24] More convincingly, Zhang *et al* have observed the gas pancake very flat gas layers directly by tapping mode AFM.[25] Interestingly, Li *et al* approved theoretically that both nanobubbles and gas pancake are all the possible existence states of gas at water/hydrophobic interface.[26] However, the stable existence of nanobubbles at water/solid interface is suffering from the classical thermodynamics.[27−31] The traditional Laplace–Young equation predicts that the pressure inside a nanobubble is extremely high (e.g., 1.4×10^6 Pa for 100 nm radius in water).[27] The lifetime predicted by conventional thermodynamics only ranges from several picoseconds to hundreds

*Project supported in part by National Natural Science Foundation of China (Grant Nos 10474109 and 10674146).
†Corresponding author. E-mail: fanghaiping@sinap.ac.cn

of microseconds,[32] which is too short to be observed experimentally.

Water molecules have many fascinating dynamical properties due to its extended hydrogen bond network. Especially, the behaviour of the gas at liquid/solid interface on the nanoscale is usually different from that in the bulk states.[33−35] We hold a view that the confliction between theory and experiments may be due to the lack of knowledge on the nanoscale gas phases at water/solid interface. It has been reported that if the densities inside nanobubbles are assumed to be large enough, the lifetime of nanobubbles increases significantly and even reaches the timescale of experimental observations.[36] Our previous molecular dynamics simulations showed that the density inside a nanobubble in bulk water, if it stably existed, is considerably large.[37] Simulations with simple Lennard–Jones liquid and hydrophobic wall by using molecular dynamics simulations also reported gas enrichment at hydrophobic interface.[3]

In this paper, we report the accumulation behaviour of gas molecules at the water/graphite interface and particularly the density of the gas by using molecular dynamics simulations. Based on the experiments,[22] which could provide continuous, high local concentration of gases, we set the initial gas concentrations in solvent water high. Here, in simulations, the accumulation states of two kinds of gases, N_2, the main content of air, and H_2 are studied. The simulation results confirm that both N_2 and H_2 can be highly accumulated together at the water/graphite interface. Two kinds of gas states are found depending on the initial ratio between number of gas molecules and square of graphite from our simulation results: gas pancake for a larger ratio and nanobubbles for a smaller ratio. At the same time, the densities of the two kinds of gas states are calculated. It is found that the densities of these two kinds of gas states are considerably larger at ambient temperature and pressure than the ambient gas states. We hope that these results will be helpful to understand the stability of nanobubbles. Moreover, the high density of hydrogen nanobubbles at water/graphite interface is expected to develop a novel hydrogen-storage method.

The outline of this paper is as follows. The computational methods and simulation results are described in Section 2. There-into, in order to verify the force field parameters, the droplet of liquid N_2 and H_2 are studied in subsection 2.1. In subsection 2.2, gas molecules enrichment at water/graphite interface is studied, which can be called a phase separation process. In subsections 2.3 and 2.4, we study two gas states at water/hydrophobic interface: gas pancake and nanobubbles, and correspondingly, represent the detailed simulation results on the densities of the two states. Conclusions of this study and remarks of the future directions are given in last section.

2. Computational methods and simulation results

The molecular dynamics simulations are carried out with Gromacs 3.2.1[38] and the SPC[39] water mode is taken. Universal Force Field (UFF),[40] as shown in Table 1, is used in our simulations. The others used in this paper, including the interactions between water molecules, are set according to Gromacs 3.2.1.[38] All simulations are performed under periodic boundary conditions in all directions. The particle-mesh Ewald method[41] is used to treat the long-range electrostatic interactions with cutoff 1 nm. All simulations are performed with an integration time step of 2 fs. The bond stretching between two covalently bonded atoms i and j is represented by a harmonic potential:

$$V(r) = \frac{1}{2}k(r-b)^2, \tag{1}$$

where k and b are force constant and standard bond length of harmonic potential respectively.

The interactions between molecules are expressed by the Lennard–Jones potential function:

$$\varphi(r) = 4\xi\left[(\sigma/r)^{12} - (\sigma/r)^6\right], \tag{2}$$

where σ and ξ are the length scale and the energy scale of the Lennard–Jones potential, respectively.

Table 1. Detailed UFF force field parameters used for the Lennard–Jones interactions.

atom type	b/nm	k/(kJ/mol·nm^2)	ε/(kcal/mol)	σ/nm
N	0.1120	1280025	0.0690	0.3260
H	0.0708	758921	0.0440	0.0392
C	0.1420	334720	0.1049	0.3430

2.1. Liquid droplet simulation

The liquid nitrogen and hydrogen droplet formation are used in our simulation to demonstrate the force field chosen to be appropriate. Molecular simulations of liquid droplet N_2 at the boiling temperature

77.3 K and liquid droplet H_2 at the boiling temperature 22 K were performed, respectively. In our series of simulations, the numbers of N_2 molecules of the systems are 1024, 1500, 2048 respectively. Initially, the nitrogen molecules form a simple cubic structure in a box with $L_x = 12\,\mathrm{nm}$, $L_y = 10\,\mathrm{nm}$, $L_z = 10\,\mathrm{nm}$, and a lattice constant $1.8405\,\sigma_\mathrm{N}$ and a maximum random displacements of $0.01\,\sigma_\mathrm{N}$ for each particle. During production runs, the simulations are weakly coupled to a Berendsen heat bath to keep the systems temperature at 77.3 K and isotropic Berendsen pressure bath to keep the systems pressure at 1 atm. Figure 1(a) shows that 1 ns is long enough to reach an equilibrium state when the densities at $t = 1\,\mathrm{ns}$ and $t = 2\,\mathrm{ns}$ have almost no difference. The density profile for different distances r from the centre of the droplet is shown in Fig.1(b).

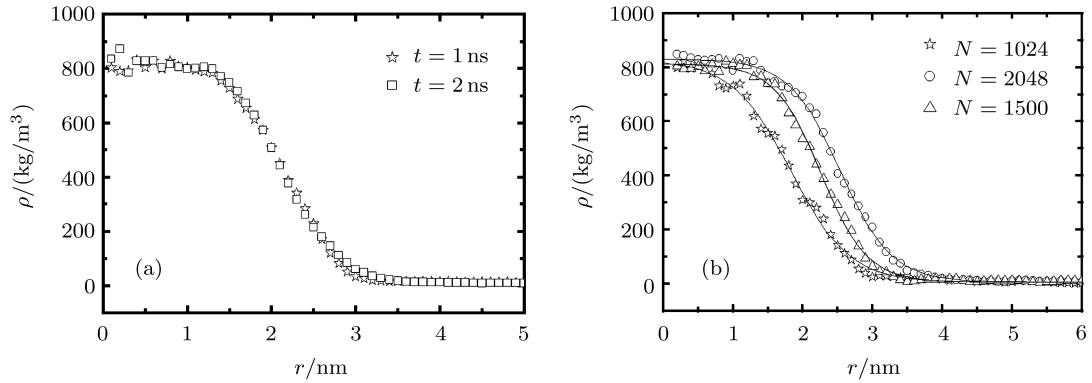


Fig.1. (a) Density profiles at $t = 1\,\mathrm{ns}$ and $t = 2\,\mathrm{ns}$ when N =1500. (b) Local density profiles for different numbers of N_2 molecules at $t = 1\,\mathrm{ns}$, where N is number of particles.

The density profile from the bulk liquid nitrogen region across the liquid–vapour interface fits a tanh function.[42]

$$\rho(r) = \frac{1}{2}\rho(\mathrm{dr})(1 - \tanh(2(r - r_\mathrm{e})/\mathrm{d})), \qquad (3)$$

where $\rho(\mathrm{dr})$ is the density of droplet, r_e is location of surface, d is thickness of surface. A fit of the equation yields a bulk liquid densities of droplet $\rho(\mathrm{dr})$ which are $829\,\mathrm{kg/m^3}$, $812\,\mathrm{kg/m^3}$, $816\,\mathrm{kg/m^3}$ for three systems respectively. Those values are very close to the experimental value of $807.4\,\mathrm{kg/m^3}$ at the boiling temperature 77.3 K[43] and a pressure 10^5 Pa.

Correspondingly, simulations with 1331, 1728, 2197 H_2 molecules are carried out keeping system temperature 22 K and pressure at 10^5 Pa. The densities at the centre of the liquid droplet are $79.0\,\mathrm{kg/m^3}$, $79.2\,\mathrm{kg/m^3}$, $80.0\,\mathrm{kg/m^3}$, for $T = 22\,\mathrm{K}$, as shown in Fig.2(b), which are close to the experimental value of $70.9\,\mathrm{kg/m^3}$ at boiling temperature 22 K[44] and a pressure 10^5 Pa.

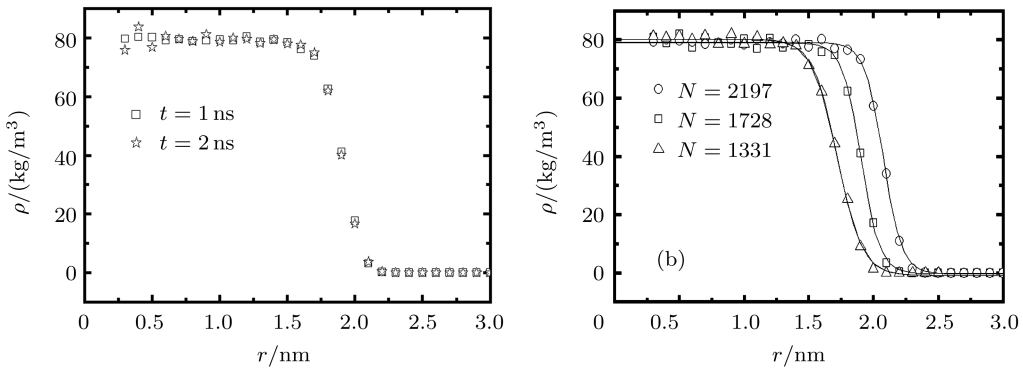


Fig.2. (a) Density profiles at $t = 1\,\mathrm{ns}$ and $t = 2\,\mathrm{ns}$ when $N = 1728$. (b) Local density profiles of H_2 at time $t = 1\,\mathrm{ns}$ at boiling temperatures 22 K, where N is particle number.

2.2. Process of gas enrichment at water/graphite interface

In this subsection, the simulations are performed to describe the spontaneous process of most of N_2 and H_2 molecules separating from bulk water and assembling at water/graphite interface, despite the gas molecules disperse in water initially. Initially, 200 N_2 and H_2 molecules are solved symmetrically in two water boxes with size $L_x = 4.20\,\text{nm}$, $L_y = 3.70\,\text{nm}$ and $L_z = 6.00\,\text{nm}$. Fixed graphite plates with size $4.06\,\text{nm} \times 3.49\,\text{nm}$ (576 carbon atoms) are located parallel to $x - y$ plane in the centre of boxes as shown in Figs.3(a) and 4(a). The simulations are performed with the NVT (constant volume-constant temperature) ensemble. Figures 3(c) and 4(c) display that the average distances between gas molecules (N_2 and H_2) and graphite are constant and independent of time after $t = 1.2\,\text{ns}$, which implicates that the systems reach equilibrium. Clearly, the equilibrium states with gas molecules assembling on the graphite are shown in Figs.3(b) and 4(b).

The next question is: what causes the gas enrichment at hydrophobic water/graphite interface? Energetically the systems benefit from the different strength of interactions between gas–water and water–water, due to water–water interactions (hydrogen bond) are stronger than that of gas–water (van der Waals interactions). Thus, the gas molecules are excluded from bulk water and adsorbed by the graphite due to van der Waals interactions between them.

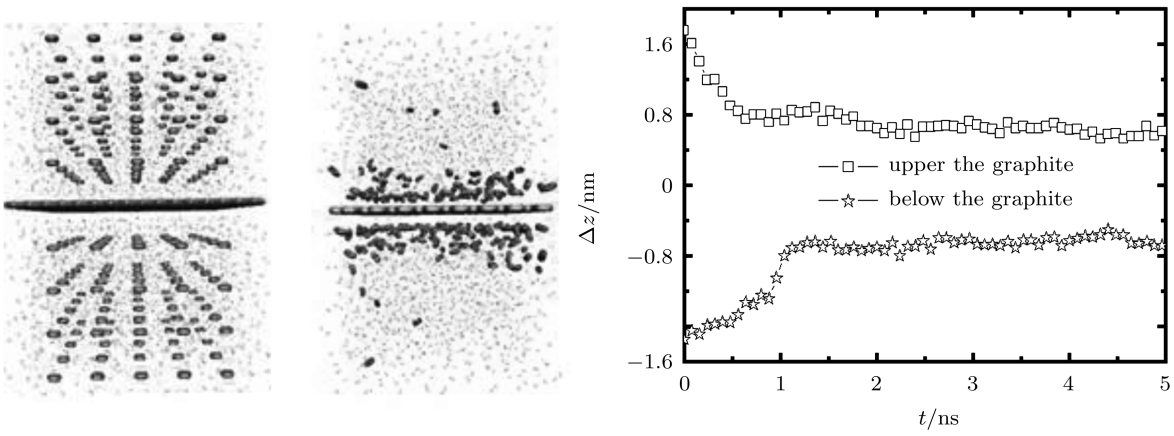


Fig.3. (a) Snapshot of initial model system. (b) Snapshot of model system when $t = 5\,\text{ns}$, with gas molecules adsorbing at graphite. (c) Average distance in z axis between N_2 molecules and graphite, where two lines indicate gas molecules upper and below the graphite both assemble at the hydrophobic interface, versus simulation time t.

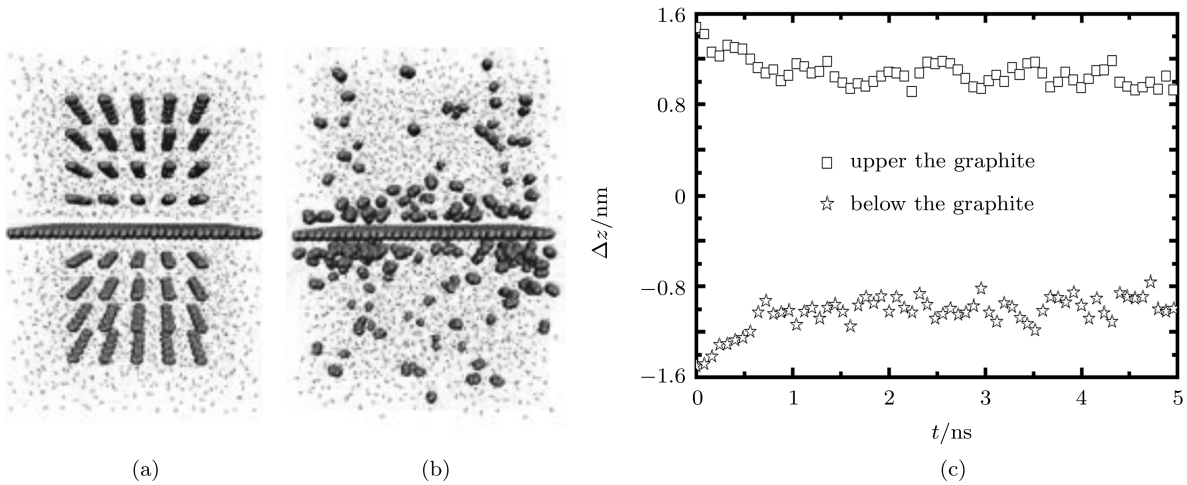


Fig.4. (a) Snapshot of initial model system. (b) Snapshot of model system when $t = 5\,\text{ns}$. (c) Average distance in z axis between H_2 molecules and graphite, where two lines indicate gas molecules upper and below the graphite both assemble at the hydrophobic interface.

2.3. Gas films (pancake-like) at water/graphite interface

Previous experimental results have shown that the contact angles for nanoscale gas bubbles are usually small[45] and the gas pancakes are very flat gas layers by tapping mode AFM.[25] Theoretically, Li *et al* approved that nanobubbles and gas pancake are all the possible existence states of gas at water/hydrophobic interface. In this subsection, numerical simulations on gas films at water/solid interface are performed and on nanobubbles in next subsection. From previous simulation results mentioned in subsection 2.2, we conclude that the N_2 and H_2 enrichment process at water/graphite interface is spontaneous process, despite the gas molecules disperse in water. On the basis of this conclusion, the initial locations of N_2 and H_2 molecules in next simulations can be localized to save simulation time.

Molecular dynamics simulations of N_2 and H_2 films (pancake-like) at water/graphite interface. A frozen graphite, which consists of four staggered sheets with an interlayer distance of 0.340 nm, with size 6.91 nm × 6.53 nm, (1734 carbon atoms per sheet) is parallel to $x-y$ plane. Additional sheets of graphite are omitted because they are not expected to have a significant influence on the water due to the employed cutoff radius of 1 nm. Initially 1800 N_2 molecules, with minimal distance 0.3 nm above the graphite, which form a simple cubic structure with a lattice constant of $1.227\sigma_{\mathrm{N}}$, are immersed in the simulation box, which is full of water molecules and has size of $L_x = 7.15$ nm, $L_y = 6.75$ nm, $L_z = 12.00$ nm. The Berendsen semi-isotropic coupling is used to maintain temperature and pressure stable around the ambient temperature (300 K) and 10^5 Pa, which allows the length of the box along the z axis (parallel to the graphite) scaled while the box dimensions in x and y fixed jointly. The time constant for scaling is set to 1000 fs, with an assumed compressibility of $4.5 \times 10^{-10}\,\mathrm{Pa}^{-1}$. After 3 ns run time, N_2 molecules begin to assemble at the hydrophobic interface and form a state with several nanometres height gas film perpendicular to the z axis (see Fig.5(a)) but yet unstable. Thus, various systems are performed by artificially removing gas molecules from gas film randomly (629, 829, 1029 N_2 molecules are removed respectively). Figure 5(b) displays the

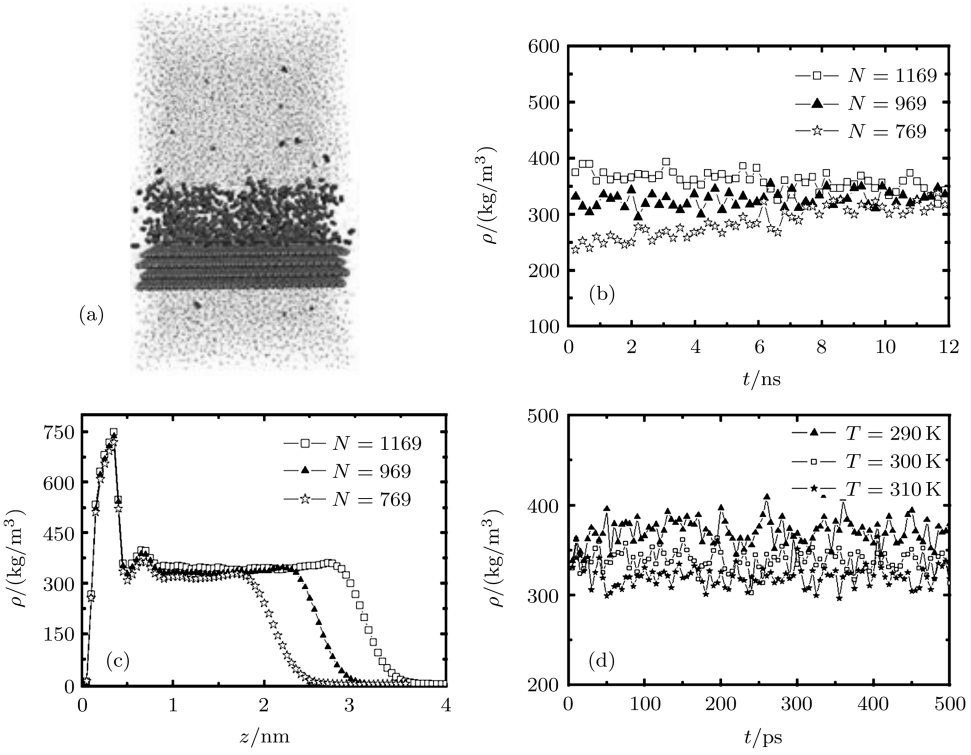


Fig.5. (a) Snapshot of the initial model system. (b) Densities versus time t starting from three different initial states, where the densities are calculated in a thickness of 1.0 nm $< z <$ 1.3 nm. (c) Density profiles in z axis of the N_2 gas films when $t = 12$ ns. (d) Density profile of gas films at different temperatures $T = 290$ K, 300 K, 310 K, respectively.

densities ρ of gas film for various systems. All of them approach a same ρ value, which indicates that all the systems reach the equilibrium. Here the densities are also computed in a thickness of 1.0 nm $< z <$ 1.3 nm. The density profiles along z axis, shown in Fig.5(c), are calculated by dividing gas film into thin slabs with Δz width ($\Delta z = 0.3$ nm), parallel to the $x - y$ plane. Obviously, two pronounced density peaks can be identified at distances of 0.35 nm and 0.70 nm with peak heights of 740 kg/m^3 and 370 kg/m^3 respectively. The first peak relates to the van der Waals interaction between the first layer molecules and graphite, and the second peak is due to the molecules near the first layer molecules. The average density is approximately 330 kg/m^3 in plateau in the region of 1.0 nm $< z <$ 1.8 nm as shown in Fig.5(c). This density value ρ is a dramatic increase of the gas in the vicinity of the hydrophobic interface when it is compared with the gas density in the bulk water, even more than 2 orders of magnitude for the gas density in the bulk water, which is consistent with that in Ref.[3]. Moreover, different N_2 molecules solved in water almost do not affect the high density in plateau, but only affect the height of gas film, as shown in Fig.5(c), which shows that the high density of gas state is quite stable during our simulation time.

Similarly, simulations with the number of H_2 2000 are performed after first 3 ns and two systems are set up subsequently by artificially removing gas molecules from gas film randomly as described previously. Figure 6(a) shows that the densities approach a same ρ value, which indicates that the two systems reach the equilibrium though starting from different initial states. From Fig.6(b), one can immediately observe two pronounced density peaks at distances of 0.3 nm and 0.6 nm, which are less than corresponding values of N_2, due to σ_H smaller than σ_N. The two peak heights are 90 and 42 kg/m^3 respectively and the average density is around 35 kg/m^3 for H_2 in plateau, which is a dramatic increase of the gas when it is compared with the gas density in the bulk water, by a factor of $\sim$30.

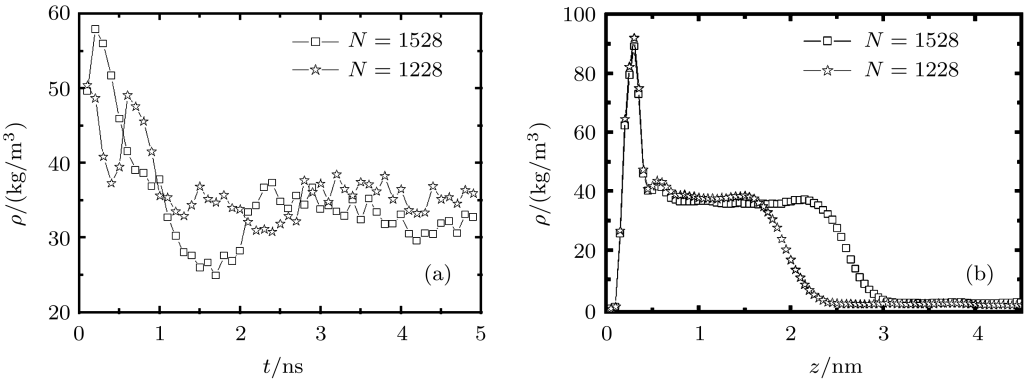


Fig.6. (a) Densities versus time t starting from two different initial states, where the densities are calculated in a thickness of 1.0 nm $< z <$ 1.3 nm. (b) Density profiles in z axis of the H_2 gas film when $t = 5$ ns.

It is necessary to examine whether environment parameters, such as temperature or pressure etc., have influences on the properties of nanobubbles. Very recently, Borkent *et al* found that the nanobubbles were not only stable under ambient conditions but also under enormous reduction of the water pressure down to –6 MPa. They denoted this phenomenon as superstability.[46] We focus on the influence of environment temperature on N_2 nanobubbles solely, due to the similarity between N_2 and H_2. Successive runs of stable gas film described before are performed for 0.5 ns at T= 290 K, 310 K, respectively, while keeping other parameters invariable. Figure 5(d) shows that different temperatures induce the different densities of bulk gas film, but the gas films states are quite stable. In addition, we find that the densities of gas film decrease as the temperature increases.

2.4. Gas nanobubbles simulation at water/graphite interface

Due to the limitation of the computer capacity, we cannot perform numerical simulations for a whole nanoscale gas bubble at water/solid interface as observed experimentally, which usually has a coverage of several tens of nanometres, together with sufficient numbers of water molecules. In this subsection, we present our study on gas bubbles with smaller size of approximately 2–3 nm at water/hydrophobic interface.

N_2 and H_2 nanobubbles simulations at water/graphite interface. In our model as shown in Fig.7(a) (water molecules are omitted), the frozen graphite with size 9.715 nm × 9.869 nm (3852 carbon atoms per sheet) is parallel to $x-y$ plane. The computation box has the size of $L_x = 10.20$ nm, $L_y = 10.20$ nm, $L_z = 6.00$ nm. Initially 800 N_2 molecules, with minimal distance 0.3 nm above the graphite, which form a simple cubic structure with a lattice constant $1.227\,\sigma_N$, are immersed in box full of water molecules. An isothermal-isobaric ensemble (normal pressure and temperature (NPT), 10^5 Pa and 300 K) is also used in simulations as aforementioned in subsection 2.3. The system is believed to reach the equilibrium when the average radius of the bottom of the bubble is independent of time as shown in Fig.7(b). The density profile along z axis is shown in Fig.7(c), with two distinct density peaks at distances around 0.35 nm and 0.70 nm. The average density is approximately 340 kg/m^3 in the region of 1.0 nm $< z <$ 2.5 nm, which is consistent with the density of N_2 films (see Fig.5(c)).

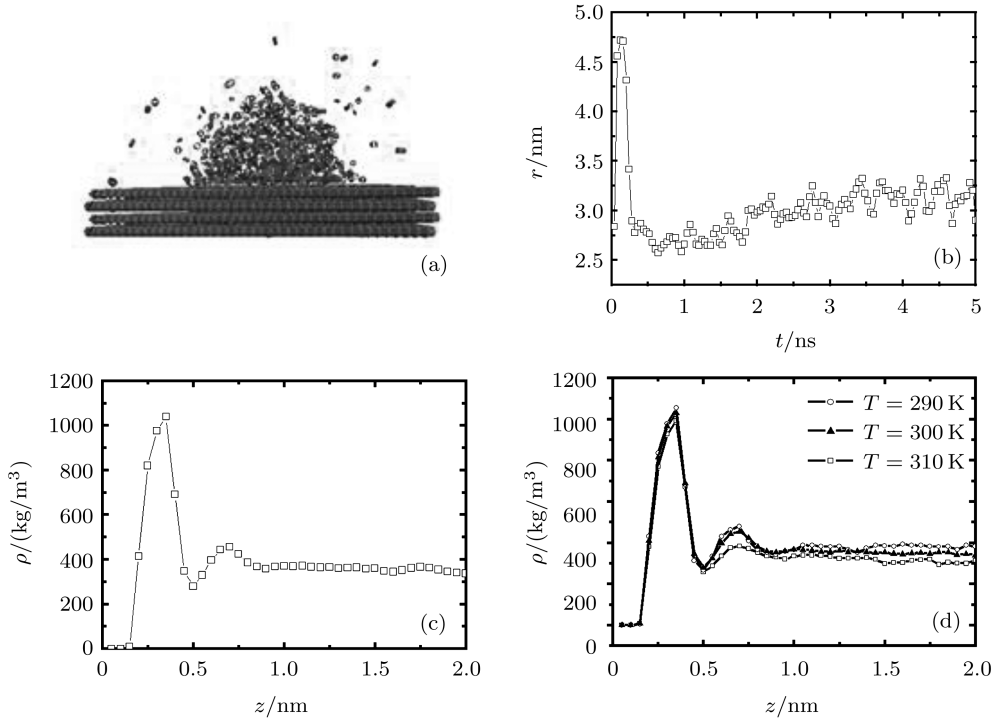


Fig.7. (a) Side view (top row) of the equilibrium state (water molecules are omitted) (b) Radius r of bottom of the N_2 nanobubble versus time t. (c) Density profile of nanobubbles in z axis. (d) Density profile of nanobubbles at different temperatures $T = 290$ K, 300 K, 310 K, respectively.

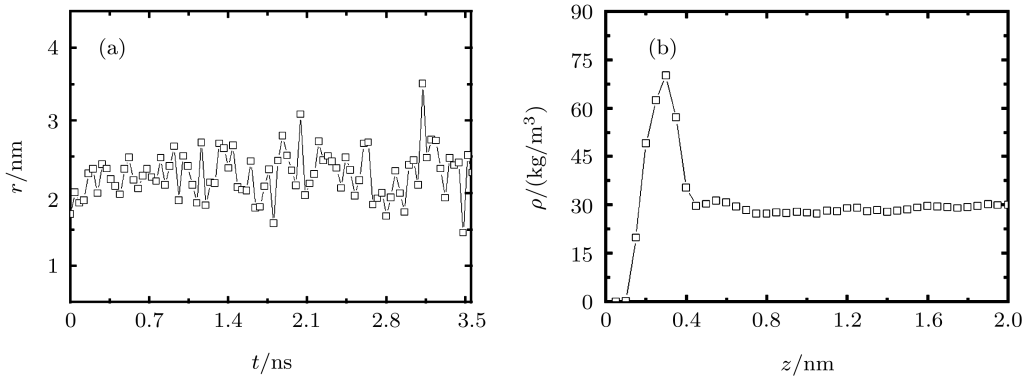


Fig.8. (a) Radius of gas bubble bottom r vs time t. (b) Density profile of nanobubble in z axis when $t = 3.5$ ns.

Similarly, the simulation for H_2 with identical water-filled box and graphite is performed under same isothermal-isobaric ensemble (NPT, 10^5 Pa and 300 K) for 3.5 ns. Figure 8(a) shows that system reaches the equilibrium, In addition, the density profiles along z axis are shown in Fig.8(b), with two density peaks at distances of 0.03 nm and 0.06 nm and average density is approximately 30 kg/m^3, which is almost consistent with the result of H_2 films in subsection 2.3.

We also verify whether the densities of gas bubbles are sensitive to environment temperatures. Parameters are set as described in subsection 2.3. After 0.5 ns equilibrium runs, we show the density profile of N_2 nanobubbles in Fig.7(d) at different temperatures $T = 290\,\mathrm{K}$, 300 K, 310 K, respectively. Obviously, temperature affects the densities of gas bubbles and the densities decrease as the temperature increases, which is consistent with previous simulation results in subsection 2.3.

3. Conclusions

Our simulations show that N_2 and H_2 molecules can separate from bulk water despite of initial dispersion in bulk water, enrich at hydrophobic water/graphite interface, and finally form two kinds of gas states: gas films (pancake-like) and nanobubbles, which are consistent with the experimental observations on the gas film (pancake-like) and surface nanobubbles. This phenomenon results from the competition between water–water interactions (hydrogen bond) and gas–water (van der Waals interactions) (the former is stronger than the latter). In addition, a pronounced density peak can be identified at distance around σ_C, which is contributed by the interaction between the first layer molecules and graphite. These results demonstrate that van der Waals interaction could help to stabilize the adsorption. Interestingly, both gas films and gas nanobubbles could hold very high densities of gas states, i.e. 41% of the density of liquid N_2, 52% of liquid H_2, respectively. In addition, we discuss the stabilities of nanobubbles at different environment temperatures.

Although it is not our intention here to present a detailed analysis of the mechanism why the densities of the two gas states are so high, it is still of value to give some qualitative explanation. On the one hand, the adsorption of gas molecules on the graphite surface is a process of heterogeneous nucleation, which makes the gas molecules easier to nucleate or adsorb on the graphite surface. On the other hand, van der Waals interaction between the gas molecules and graphite surface favours the adsorption of gas molecules, and at the nanometre scale, as in our simulation, there are only several absorbed gas molecules layers. According to the gas adsorption theory, the density of the initial several layers is very high due to the strong adsorption. Therefore, the high densities of the two states in our simulations are conceivable. Detailed investigation on this issue is underway.

We should emphasize that the time duration for each simulation is still very short. From our study, we cannot predict the longtime stability of the nanobubbles and gas pancakes. Moreover, the extra high-densities of the N_2 and H_2 molecules inside the gas pancakes and nanobubbles are unexpected and contradicted to convectional knowledge although it has been argued that the large density is helpful to the understanding of the stability.[36] This should be further tested by experiments. If this has been demonstrated, high coverage of hydrogen nanobubbles can be used as a new potential technique for hydrogen storage at ambient temperature and pressure.

Acknowledgment

We thank Lu Hang-Jun, Zhang Li-Juan, Yi Hou-Hui, Tu Yu-Song and Zhou Bo for helpful discussions and comments. This work was supported is part by the Shanghai Supercomputer Center of China.

References

[1] Ball P *Nature* 2003 **423** 25
[2] Smeets R M M, Keyser U F, Wu M Y, Dekker N H and Dekker C 2006 *Phys. Rev. Lett.* **97** 088101
[3] Dammer S M and Lohse D 2006 *Phys. Rev. Lett.* **96** 206101
[4] Christenson H K and Claesson P M 2001 *Adv. Colloid Interface Sci.* **91** 391
[5] Attard P 2003 *Adv. Colloid Interface Sci.* **104** 75
[6] Meyer E E, Rosenberg K J and Israelachvili J 2006 *Proc. Natl. Acad. Sci.* USA **103** 15739
[7] Wang X D, Dong P, Chen S L and Yi G Y 2007 *Acta Phys. Sin.* **56** 3017 (in Chinese)
[8] Doshi A D, Watkins E B, Israelachvili J N and Majewski Jaroslaw 2005 *Proc. Natl. Acad. Sci.* USA **102** 9458
[9] Verwey E J W and Overbeek J T G 1948 *Theory of the Stability of Lyophobic Colloids* (New York: Elsevier)

[10] Chiara N, Drew R E, Elmar B, Hans-Jürgen B and Vincent S J C 2005 *Rep. Prog. Phys.* **68** 2859
[11] de Gennes P G 2002 *Langmuir* **18** 3413
[12] Parker J L, Claesson P M and Attard P 1994 *J. Phys. Chem.* **98** 8468
[13] Lou S T, Ouyang Z Q, Zhang Y, Li X J, Hu J, Li M Q, and Yang F J 2000 *J. Vac. Sci. Technol.* B **18** 2573
[14] Zhang X H, Zhang X D, Lou S T, Zhang Z X, Sun J L and Hu J 2004 *Langmuir* **20** 3813
[15] Tyrrell J W G and Attard P 2001 *Phys. Rev. Lett.* **87** 1761041
[16] Agrawal A P J, Ryu D Y, Hammond P T, Russell T P and McKinley G H 2005 *Nano Lett.* **5** 1751
[17] Zhang X H, Maeda N and Craig V S J 2006 *Langmuir* **22** 5025
[18] Zhang X H, Li G, Wu Z H, Zhang X D and Hu J 2005 *Chin. Phys.* **14** 1774
[19] Lou S T, Gao J X, Xiao X D, Li X J, Li G L, Zhang Y, Li M Q, Sun J L and Hu J 2001 *Chin. Phys.* **10** S108
[20] Switkes M and Ruberti J W 2004 *Appl. Phys. Lett.* **84** 4759
[21] Steitz R, Gutberlet T, Hauss T, Klosgen B, Krastev R, Schemmel S, Simonsen A C and Findenegg G H 2003 *Langmuir* **19** 2409
[22] Zhang L J, Zhang Y, Zhang X H, Li Z X, Shen G X, Ye M, Fan C H, Fang H P and Hu J 2006 *Langmuir* **22** 8109
[23] Schwendel D, Hayashi T, Dahint R, Pertsin R, Grunze M and Steitz R 2003 *Langmuir* **19** 2284
[24] Jensen T R, Jensen M Ø, Reitzel N, Balashev K, Peters G H, Kjaer K and Bjørnholm T 2003 *Phys. Rev. Lett.* **90** 086101
[25] Zhang X H, Zhang X D, Sun J L, Zhang Z X, Li G, Fang H P, Xiao X D, Zeng X C and Hu J 2007 *Langmuir* **23** 1778
[26] Li Z X, Zhang X H, Zhang L J, Zeng X C, Hu J and Fang H P 2007 *J. Phys. Chem.* B **111** 9325
[27] Holmberg M, Kuhle A, Garnaes J, Mrch K A and Boisen A 2003 *Langmuir* **19** 10510
[28] Pashley R M, Rzechowicz M, Pashley L R and Francis M J 2005 *J. Phys. Chem.* B **109** 1231
[29] Maeda N, Rosenberg K J, Israelachvili J N and Pashley R M 2004 *Langmuir* **20** 3129
[30] Lohse D 2003 *Phys. Today* **56** 36
[31] Granick S, Zhu Y X and Lee H 2003 *Nat. Mater.* **2** 221
[32] Ljunggren S and Eriksson J C 1997 *Colloids and Surf.* A **129–130** 151
[33] Hummer G, Rasalah J C and Noworyta J P 2001 *Nature* **414** 188
[34] Li J Y, Yang Z X, Fang H P, Zhou R H and Tang X W 2007 *Chin. Phys. Lett.* **24** 2710
[35] Zhou X Y and Lu H J 2007 *Chin. Phys.* **16** 0335
[36] Zhang L J, Chen H, Li Z X, Fang H P and Hu J *Science in China* Series G—Physics and Astronomy **51** 219
[37] Fang H P and Hu J 2006 *Nucl. Sci. Technol.* **17** 71
[38] Lindahl E, Hess B and van der Spoel D 2001 *J. Mol. Model.* **7** 306
[39] Berendsen H J C, Postma J P M, van Gunsteren W F and Hermans J In *Pullman, B (ed) 1981 Intermolecular Forces* (Dordrecht: Reidel) p331
[40] Rappé A K, Casewit C J, Colwell K S, Goddard III W A and Skiff W M 1992 *J. Am. Chem. Soc.* **114** 10024
[41] Darden T A, York D M and Pedersen L G 1993 *J. Chem. Phys.* **98** 10089
[42] Werder T, Walther J H, Jaffe R L, Halicioglu T and Koumoutsakos P 2003 *J. Phys. Chem.* B **107** 1345
[43] http://www.tkb-4u.com/articles/consumables/whatisnit-rogen/whatisnitrogen.php
[44] http://www.speclab.com/elements/hydrogen.htm
[45] Simonsen A C, Hansen P L and KlÖsgen B 2004 *J. Colloid. Interface. Sci.* **273** 291
[46] Bram M Borkent, Stephan M Dammer, Holger Schönherr, G. Julius Vancso and Detlef Lohse 2007 *Phys. Rev. Lett.* **98** 204502